The *SPA2* Protein of Yeast Localizes to Sites of Cell Growth

Michael Snyder

Department of Biology, Yale University, New Haven, Connecticut 06511

Abstract. A yeast gene, *SPA2*, was isolated with human anti–spindle pole autoantibodies. The *SPA2* gene was fused to the *Escherichia coli trpE* gene, and polyclonal antibodies were prepared to the fusion protein. Immunofluorescence experiments indicate that the *SPA2* gene product has a sharply polarized distribution in yeast cells. In budded cells the SPA2 protein is present at the tip of the bud; in unbudded cells, it is localized to one edge of the cell. When a-cells are induced to form schmoos with α-factor, the SPA2 protein is found at the tip of the schmoo. These areas of SPA2 localization correspond to cellular sites expected to be involved in bud formation and/or cell growth.

The SPA2 antigen is present in a-cells, α-cells, and a/α-diploid cells, but is absent in mutant cells in which the *SPA2* gene has been disrupted. *spa2* mutant cells are viable, but display defects in the direction and control of cell growth. Compared to wild-type cells, *spa2* mutant cells have slightly altered budding patterns. Entry into stationary phase is impaired for *spa2* mutants, and mutants with one particular allele, *spa2-7*, form multiple buds under nutrient-limiting conditions. Thus, *SPA2* is a newly identified yeast gene that is involved in the direction and control of cell division, and whose gene product localizes to the site of cell growth.

THE generation and maintenance of cell polarity is a process pertinent to most eukaryotes. Cellular morphogenesis of many cell types depends on polarized cell growth, and the development and differentiation of multicellular organisms requires accurate polarized cell divisions at crucial times in development. Little is known about the molecules that specifically reside in regions of cell growth or the molecular mechanisms that govern polarized growth and division.

The budding yeast, *Saccharomyces cerevisiae*, exhibits polarized cell growth. In late Gl of the cell cycle, bud synthesis initiates at a site on the edge of the cell. Bud growth continues principally at the bud tip until the size of the bud nears that of the mother cell (Byers, 1981; Adams and Pringle, 1984). Cytological observations suggest that microtubules may play an important role in bud formation and/or growth. In budded cells, cytoplasmic microtubules extend into the bud. In unbudded Gl cells, cytoplasmic microtubules emanate from the yeast spindle pole body and have been postulated to direct the site of bud formation (see Byers and Goetsch, 1975; Byers, 1981). A full complement of microtubules is not essential for bud formation because tubulin mutants and nocodazole-treated cells are still able to form buds (Huffaker et al., 1988; Jacobs et al., 1988). However, microtubules may still play an important role either in directing bud site formation and/or in augmenting cell growth.

S. cerevisiae is also useful for studying polarized cell division because yeast controls the directionality of each cell division. The pattern of bud formation occurs in a well-defined fashion depending upon the mating type and pedigree of the cell (Freifelder, 1960). Haploid a- and α-cells bud in an axial fashion, in which the new bud forms adjacent to the old bud site (Fig. 1). For diploid a/α-cells, the pattern of budding is dependent upon the pedigree of the cell involved. Mother cells, i.e., cells that have given birth to one or more cells, bud in an axial pattern similar to that of haploids. New daughter cells, however, bud in a polar fashion, with the new bud forming opposite the old birth scar. The molecular mechanism that determines cell polarity is not understood at present.

The decision to initiate cell growth is made in late Gl of the cell cycle, at a point called *Start* (Hartwell, 1974). Once cells have completed Start they are committed to progress through the remainder of the cell cycle. This commitment is dependent on a variety of factors (reviewed in Pringle and Hartwell, 1981). Among the factors are both positive and negative signals. First, cells must reach a critical size; cells that are too small will not enter the mitotic cell cycle. Second, when nutrients are limiting, cells will arrest and enter stationary phase. Alternatively, when particular nutrients are limiting, diploid cells can also exit the mitotic cell cycle and begin sporulation. Finally, in the presence of mating hormones, haploid cells of the opposite mating type will also arrest before Start.
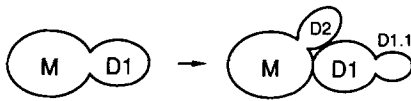
In this paper a yeast gene is described called *SPA2* (for

---

1. *Abbreviations used in this paper*: cMor, centiMorgans; β-gal, β-galactosidase; SPA, spindle pole antigen.

Haploid- Axial Budding
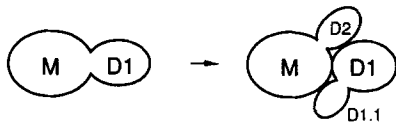
Diploid- Axial/Polar Budding

Figure 1. Budding patterns of haploid and diploid yeast cells. Haploid mother (*M*) and daughter (*D1*) cells form new buds (*D2* and *D1.1*, respectively) adjacent to the old bud site. Diploid mother cells exhibit the same pattern as haploid mothers, but diploid daughter cells bud opposite the old bud site.

Spindle Pole Antigen) that is important for cell growth and bud formation. The *SPA2* gene product localizes to the site of cell growth, and mutations in the *SPA2* gene lead to defects in both the control and the direction of cell division.

Materials and Methods

Yeast Strains/General Methods

All yeast strains are in an isogenic S288c background; a list is presented in Table I. YPD media and general genetic manipulations are as described in Sherman et al. (1986). General cloning procedures are as described in Davis et al. (1980), Maniatis et al. (1982), and Snyder and Davis (1988).

Isolation and Disruption of the SPA2 Gene

The *SPA2* gene was isolated by immunoscreening a yeast genomic DNA expression library with the 5051 anti–spindle pole autoantibody (Tuffanelli et al., 1983) as described in Snyder and Davis (1988). Transplason mutagenesis of λSPA2.2 with mini-Tn10 transposons containing the *URA3* gene is

detailed in Snyder et al. (1986). Substitution of the mutated *SPA2* gene for the genomic copy was accomplished by one step gene transplacement (Rothstein, 1983). 2 μg of a minipreparation of mutagenized phage DNA (Snyder et al., 1986) was partially digested with Eco RI and transformed into diploid yeast strain Y270 using the lithium acetate procedure of Ito et al. (1983). The resulting transformants were sporulated and substitution at the *SPA2* locus was checked in haploid progeny by genomic DNA gel blot analysis using *SPA2* gene probes. Crosses of Ura^+ spa2-7 and spa2-8 mutant cells with other Ura^+ spa2-7 and spa2-8 mutant cells always showed 4:0 segregation of the *URA3* marker.

The *spa2-Δ1* allele was constructed by cloning a 7.4-kb Sal I/Kpn I DNA fragment containing the *SPA2* gene into a yeast centromeric plasmid that contains a *TRP1* gene. The resulting plasmid is called p188. A 1.4 kb *TRP1/ARS1* Eco RI fragment of YRp7 was subsequently substituted for the internal 2.2-kb Sph I fragment of the *SPA2* gene. To perform this last step, the ends of the *TRP1/ARS1* fragment and the appropriate p188 fragment had first been made flush using the large fragment of DNA polymerase I. Diploid yeast cells were transformed with a linear DNA fragment containing the *spa2-Δ1* allele and sporulated. Substitution at the *SPA2* locus was confirmed in haploid progeny by three criteria: (*a*) genomic gel blot analysis and tetrad analysis as described above, (*b*) by the failure of *spa2-Δ1* mutant cells to stain with anti-SPA2 antibodies using indirect immunofluorescence, and (*c*) by the failure of proteins from *spa2* mutant cells to react with affinity-purified anti-SPA2 antibodies using immunoblot analysis.
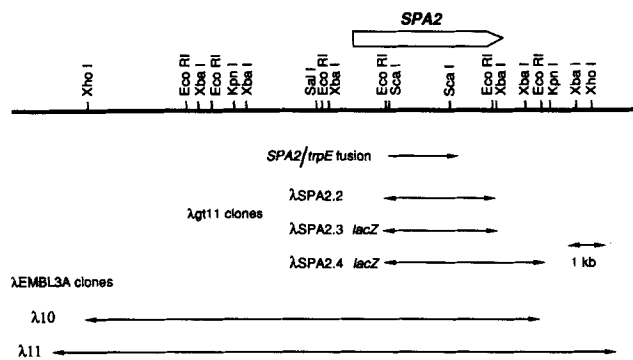
Production of Antibodies to the SPA2 Protein

A 1.9-kb Sca I fragment derived from λ10 (Fig. 2) was cloned into the Sma I site of pATH11 and introduced into *Escherichia coli* strain CAG456 (Baker et al., 1984). An overnight culture of this strain was grown in M9 media containing 50 μg/ml ampicillin and 20 μg/ml tryptophan. Four cultures were prepared that contained 2.5 ml of the fresh overnight culture diluted into 110 ml of M9 media (lacking ampicillin and tryptophan) in a 2 liter flask, and the cultures were grown for 3–4 h at 30°C. Expression of the fusion protein was induced by the addition of 1.5 ml of 1 mg/ml indoleacrylic acid to each flask, and the incubation was continued for 4 h more at 30°C. Cells were next incubated at 4°C for 2–10 h, then pelleted at 7,500 *g* for 3 min, and washed once with 20 ml 50 mM Tris-HCl, pH 7.5, 5 mM EDTA (solution A). The cell pellet was resuspended in 20 ml solution A containing 3 mg/ml lysozyme and incubated on ice for 2–3 h. 1.4 ml 5 M NaCl and 1.5 ml of 10% NP-40 were added, and after 30 min the sample was sonicated briefly to lyse the cells. The insoluble material was collected by centrifugation at 12,000 *g* for 10 min at 0°C, and the pellet washed twice with 20 ml 10 mM Tris-HCl, pH 7.5, followed by 12,000 *g* centrifugation as above after each wash. The final pellet was dissolved in 0.8 ml SDS lysis buffer (Laemmli, 1970). 0.5–2 mg of SPA2/trpE fusion protein was recovered per

Table I. Strain list

S288c isogenic background						
Y90	*a ura3-52*	*lys2-801*	*ade2-101*	*trp1-901*		
Y93	*a ura3-52*	*lys2-801*	*ade2-101*	*trp1-901*	*his3-Δ200*	
Y216	*a ura3-52*	*lys2-801*	*ade2-101*	*trp1-901*	*spa1-1/TRP1*	
Y197	*a ura3-52*	*lys2-801*	*ade2-101*	*trp1-901*	*his3-Δ200*	*spa1-2/URA3*
Y415	*a ura3-52*	*lys2-801*	*ade2-101*	*trp1-901*	*his3-Δ200*	*spa2-7/URA3*
Y416	*α ura3-52*	*lys2-801*	*ade2-101*	*trp1-901*	*his3-Δ200*	*spa2-7/URA3*
Y420	*a ura3-52*	*lys2-801*	*ade2-101*	*trp1-901*	*his3-Δ200*	*spa2-8/URA3*
Y421	*α ura3-52*	*lys2-801*	*ade2-101*	*trp1-901*	*his3-Δ200*	*spa2-8/URA3*
Y548	*a ura3-52*	*lys2-801*	*ade2-101*	*trp1-901*	*his3-Δ200*	*spa2-Δ1/TRP1*
Y549	*α ura3-52*	*lys2-801*	*ade2-101*	*trp1-901*	*his3-Δ200*	
Y550	*α ura3-52*	*lys2-801*	*ade2-101*	*trp1-901*	*his3-Δ200*	*spa2-Δ1/TRP1*
Y551	*a ura3-52*	*lys2-801*	*ade2-101*	*trp1-901*	*his3-Δ200*	
Y270 (YNN318)	*a ura3-52*	*lys2-801*	*ade2-101*	*trp1-901*	*his3-Δ200*	
	α ura3-52	*lys2-801*	*ade2-101*	*trp1-901*	*his3-Δ200*	
Y376	*a ura3-52*	*lys2-801*	*ade2-101*	*trp1-901*	*his3-Δ200*	*spa1-1*
	α ura3-52	*lys2-801*	*ade2-101*	*trp1-901*	*HIS3*	*spa1-1*
Y457	*a ura3-52*	*lys2-801*	*ade2-101*	*trp1-901*	*his3-Δ200*	*spa2-7/URA3*
	α ura3-52	*lys2-801*	*ade2-101*	*trp1-901*	*his3-Δ200*	*spa2-7/URA3*
Y556	*a ura3-52*	*lys2-801*	*ade2-101*	*trp1-901*	*his3-Δ200*	*spa2-Δ1/TRP1*
	α ura3-52	*lys2-801*	*ade2-101*	*trp1-901*	*his3-Δ200*	*spa2-Δ1/TRP1*

The strains Y548–Y551 are the progeny of a single meiosis.

Xho I

Eco RI
Xba I
Eco RI
Kpn I
Xba I

Sal I
Sca RI
Eco RI
Xba I

Eco RI
Sca I

Sca I

Eco RI
Xba I

Xba I
Eco RI
Kpn I

Xba I
Xho I

SPA2/trpE fusion ⟶

λSPA2.2 ⟶

λgt11 clones

λSPA2.3 lacZ ⟶

λSPA2.4 lacZ ⟶ 1 kb

λEMBL3A clones

λ10 ⟵⟶

λ11 ⟵⟶

Figure 2. Restriction map of the *SPA2* locus. The *SPA2* open reading frame is indicated by the open box; the extent of the open reading frame is crudely estimated from protein gel data and the positions of the endpoints are imprecise (see Discussion). Restriction endonuclease sites are also indicated on the map; Sca I sites were not mapped outside of the *SPA2* open reading frame. The extent of the *SPA2*λgt11- and λEMBL3A-cloned DNA inserts are shown beneath the map. The 1.9-kb Sca I fragment was inserted into the pATH11 vector which allowed the production of a 107-kD SPA2/trpE fusion protein.

liter of culture. The fusion protein was electroeluted from preparative SDS-7% polyacrylamide gels (Laemmli, 1970) and precipitated with acetone. 200 μg was injected into a rabbit with boost injections every 3-6 wk. The titer of the serum was monitored with immunoblots (Burnette, 1981) containing SPA1/trpE, SPA2/trpE, SPA1/β-galactosidase (β-gal), SPA2/β-gal, β-gal, and trpE proteins. SPA1/β-gal and SPA2/β-gal fusion proteins were prepared from λ*SPA1.1* and λ*SPA2.3* clones (Snyder and Davis, 1988) using *E. coli* strain CAG456 and previously described procedures (Snyder et al., 1987). Affinity-purified antibodies to the SPA2 protein were prepared by incubating 200-250 μg of SPA2/trpE fusion protein with a 1.7-cm² piece of nitrocellulose overnight at 4°C. The filter was washed with TBS (150 mM NaCl, 50 mM Tris-HCl) and incubated with TBS containing 3% BSA for 2 h. The filter was next incubated overnight at 4°C with rabbit serum (0.4 ml diluted with 0.8 ml TBS), and the filter was subsequently washed five to six times with TBS. Bound antibody was eluted with a 0.2 M glycine solution, pH 2.5, neutralized as described (Snyder et al., 1987), and dialyzed against TBS for 8 h. 1:100 dilutions in TBS plus 1% BSA were used for immunofluorescence, and 1:300 dilutions in TBS plus 20% fetal calf serum were used for immunoblots.

Yeast Immunoblot Analysis

Total yeast cellular proteins were prepared as follows: haploid yeast cultures were grown in 5 ml YPD to OD (600) ∼1, collected by centrifugation, and washed once with distilled water. Cells were resuspended in 50 μl double distilled H₂O and 0.5 ml SDS lysis buffer was added. (SDS lysis buffer = 40 mM Tris-HCl [pH6.8], 1% SDS, 50 mM dithiothreitol, 50% wt/vol urea, and 2 μg/ml each of chymostatin, leupeptin, antipain, and pepstatin.) 0.4 ml of acid-washed glass beads were added, and the sample was vortexed at high speed for 5-10 min. The sample was next heated at 105°C for 2 min, centrifuged for 5 min at 13,000 g, and 5 μl was loaded onto a 5-16% polyacrylamide-SDS gel (Laemmli, 1970). The integrity of the protein preparation and the relative amount of protein for each sample was accessed by comparing the different lanes after staining the gel with Coomassie blue. Immunoblots were prepared and probed with affinity-purified anti-SPA2 antibodies as described (Snyder and Davis, 1988).

Immunofluorescence

Indirect immunofluorescence using fixed yeast cells was performed as described in Kilmartin and Adams (1984), Adams and Pringle (1984), and Bond et al. (1986). A human anti-microtubule autoantiserum that reacts with mitotic spindles of yeast and mammalian cells was used in the double immunofluorescence experiments. Bound rabbit antibodies were detected with affinity-purified, fluorescein-conjugated goat anti-rabbit antibodies; bound human antibodies were identified with affinity-purified rhodamine-conjugated goat anti-human antibodies. a-Cells were arrested by adding

α-factor (3 μg/ml final concentration) to a culture grown in YPD media to OD (600) ∼0.5. 50 min later α-factor treatment was repeated, and after an additional 40 min cells were fixed for immunofluorescence. For immunofluorescence on mating cells, a-cells grown to OD (600) ∼0.5 were mixed with α-cells grown to the same density, and harvested 5 h later.

Polarity of Budding

The budding pattern of yeast cells was determined by isolating individual budded cells from an exponentially growing culture, aligning them on a YPD plate by micromanipulation, and inspecting the cells every 5-15 min through a dissecting microscope. These experiments were carried out at 24°C. After the mother cell and the daughter cell had budded, the cells were separated, and the observation continued. The position of the new bud was determined relative to the old bud. Deviations from the axial budding pattern of mother cells, particularly in diploids, were observed when using either (a) random cells from a growing population, or (b) cells starting growth from stationary phase, or (c) cells in which the mother cell had already undergone several divisions. Therefore, the results of budding from new mother cells and daughter cells are presented below and were quite reproducible. For haploid daughter cells in our strains, the direction of budding can sometimes be difficult to determine because the mother cell usually has budded twice before the time the daughter buds. The extra buds of the mother can perturb the orientation of daughter cell, thereby creating scoring inaccuracies for daughter budding patterns. For diploids, the mother cell only buds once before the daughter buds and the interference is minimal.
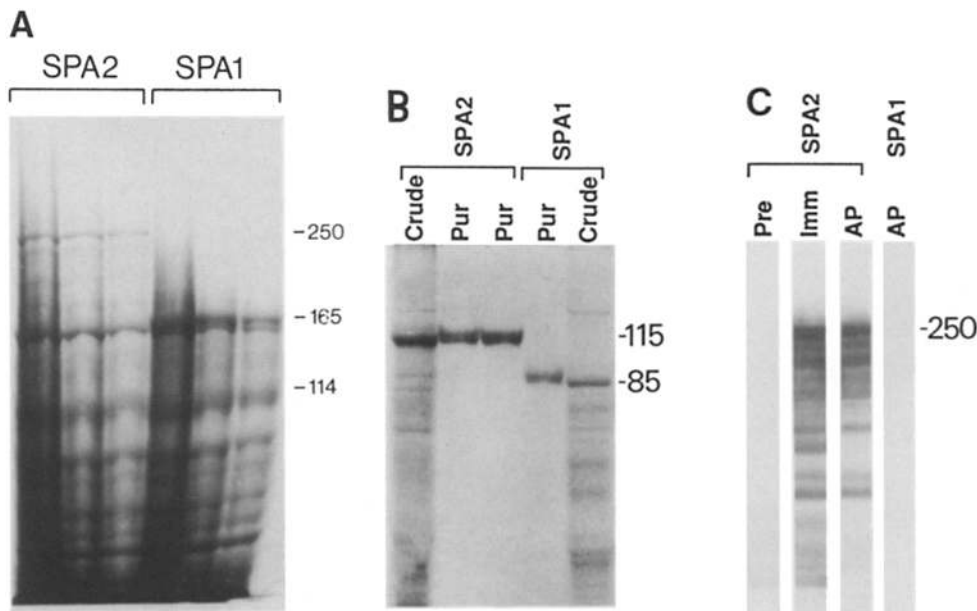
Results

Identification of the SPA2 Gene

The *SPA2* gene of *S. cerevisiae* was identified during a search for yeast genes related to the mammalian spindle pole (Snyder and Davis, 1988). A λgt11 yeast genomic DNA expression library was screened with human anti-spindle pole autoantibodies, and three λgt11 *SPA2* clones were identified and characterized (Fig. 2). The λgt11 clones λ*SPA2.3* and λ*SPA2.4* encode large β-gal fusion proteins, estimated to be >250 kD, of which 114 kD is β-gal (Fig. 3 *A*). Thus, the *SPA2* gene contains a long open reading frame. Proteins encoded by λ*SPA2.3* can be used to affinity purify antibodies from a human anti-spindle pole antiserum. These affinity-purified antibodies recognize the mammalian spindle pole by immunofluorescence, demonstrating that the SPA2 protein has epitopes in common with the mammalian spindle pole (Snyder and Davis, 1988).

The SPA2 Gene Maps to Chromosome XII

Gel blot analysis of genomic DNA has indicated that *SPA2* is a single copy gene in yeast (Snyder and Davis, 1988). Resolution of yeast chromosomal DNA by pulsed-field gel electrophoresis followed by hybridization with *SPA2* DNA probes mapped the *SPA2* gene to chromosome XII (Snyder and Davis, 1988). Initial genetic crosses indicated that *SPA2* is linked to a centromere. We therefore tested whether *SPA2* is linked to *ASP5*, which is known to reside close to the centromere on chromosome XII. A *spa2* mutant gene containing a *URA3* marker (see below) was genetically mapped relative to *asp5* using standard tetrad analysis (Sherman et al., 1986; Table II). In the same crosses, the position of the *SPA2* gene was mapped relative to the centromere using the *met14* marker. From this analysis, *spa2* was found to lie ∼35 centiMorgans (cMor) from *asp5* and 21 cMor from the centromere. *ASP5* was determined to be 21 cMor from the centromere, in reasonable agreement with published results (18.2 cMor; Mortimer and Schild, 1980). Thus, we conclude that

A

SPA2   SPA1

-250

-165

-114

B

SPA2   SPA1

Crude | Pur | Pur | Pur | Crude

-115

-85

C

SPA2   SPA1

Pre | Imm | AP | AP

-250

Figure 3. (A) β-gal fusion proteins of *SPA1* and *SPA2* λgt11 clones. *E. coli* lysates containing β-gal fusions were prepared from λ*SPA2.3* and λ*SPA1.1* as described in Snyder et al. (1987). Approximately 30, 20, and 10 μg of protein lysates of each sample were loaded (from left to right) and separated on 5% polyacrylamide-SDS gels (Laemmli, 1970), and the gel stained with Coomassie blue. The estimated sizes of the fusion proteins is indicated on the right; *114*, the migration position of the β-gal marker. Identification of the SPA1 and SPA2 fusion proteins was confirmed by preparing immunoblots of a similar gel and probing with 5051 anti-spindle pole autoantibodies. The indicated bands react strongly with the antiserum. (B) trpE fusion proteins. SPA2/trpE and SPA1/trpE fusion proteins were prepared as described in Materials and Methods, separated on a 5% polyacrylamide-SDS gel, and the gel was stained with Coomassie blue. The samples for SPA2 are as follows: *Crude*, SPA2/trpE-insoluble protein preparation; *Pur*, two gel-purified SPA2/trpE protein preparations. The sample on the left is slightly contaminated with *E. coli* RNA polymerase and has not been used further. SPA1 samples are as follows: *Pur*, gel-purified SPA1/trpE protein; *Crude*, crude SPA1/trpE-insoluble protein preparation. (C) Immunoblots of SPA2/β-gal fusion proteins. Crude lysates of SPA2/β-gal and SPA1/β-gal fusion proteins were prepared using λ*SPA2.3* and λ*SPA1.1* clones, respectively, and immunoblots of these proteins probed with SPA2 antibodies. Equal amounts of proteins are on each blot. (*SPA2*) Protein lysates of SPA2/β-gal fusions probed with preimmune serum (*Pre*), immune serum (*Imm*), and affinity-purified anti-SPA2 antibodies (*AP*). Extensive degradation of the SPA2/β-gal fusion proteins occurs in *E. coli*, hence many smaller bands exist. (*SPA1*) Protein lysates of SPA1/β-gal fusion protein probed with affinity-purified anti-SPA2 antibodies. The anti-SPA2 antibodies do not cross-react with the SPA1/β-gal protein, hence the immunoblot with the SPA1/β-gal fusion serves as a negative control for these experiments.

SPA2 lies on the left side of chromosome XII, and the order of the genes is *SPA2-CENXII-ASP5*.

The SPA2 Gene Encodes a Large Polypeptide

To investigate the function of *SPA2*, antibodies were raised to the *SPA2* gene product to allow immunolocalization of this

Table II. Distance of spa2 Relative to asp5 and the Centromere Marker met14

Markers	PD	NPD	TT	FDS	SDS	cMor
spa2/URA3–asp5	12	0	29	–	–	35
spa2/URA3–met14	–	–	–	22	20	
spa2/URA3–CENXII						21
asp5–met14	–	–	–	24	23	
asp5–CENXII						21

Diploid strain Y415 × Y487 which is heterozygous for *asp5*, *met14*, and *spa2–7* (marked by *URA3*) was sporulated and the segregation pattern analyzed in tetrads containing 4:0 and 3:1 viable/dead spores. For the three spore-viable tetrads, the genotype of the missing spore was deduced assuming a 2:2 segregation pattern of the markers. Similar results were obtained for four- and three-spore viable tetrads. The *asp5–spa2* distance was calculated using the formula 1/2 tetratypes/total *n* of tetrads × 100 (Mortimer and Schild, 1980). The *spa2–CENXII* and *asp5–CENXII* distances were calculated using the *met14* marker and the formula 1/2 second division segregation (*SDS*)/total number of tetrads × 100, and subtracting the published distance of *met14* from the centromere (2.6 cM; Mortimer and Schild, 1980). The strain also carries a 50-kb minichromosome containing *TRP1*; analysis of the *TRP1* marker yielded results comparable to those with the *met14* data reported in the Table. PD, parental ditype; NPD, nonparental ditype; TT, tetratype; FDS, first division segregation; SDS, second division segregation; cMor, centiMorgans.

protein in yeast. A 1.9-kb open reading frame segment of the *SPA2* gene was fused to the *E. coli trpE* gene, permitting production of a fusion protein containing 70 kD of SPA2 and 37 kD of trpE sequence. The fusion protein was overproduced in *E. coli* and high titer polyclonal antibodies prepared (Fig. 3 *B*). Affinity-purified antibodies specific for the SPA2/trpE fusion protein were prepared as described in the Materials and Methods section. These affinity-purified antibodies react strongly with the β-gal fusion proteins encoded by λ*SPA2.3* and λ*SPA2.4*, but do not react with either SPA1/β-gal fusion proteins or *E. coli* proteins (see Fig. 3 *C*).

Immunoblots of total yeast cellular proteins were probed with affinity-purified anti-SPA2 antibodies. As shown in Fig. 4, a yeast protein of ∼180 kD molecular mass is recognized by the antibody probe. Several minor species of lower molecular mass are also detected; we suspect that these are likely to be degradation products as their presence diminishes under conditions that reduce proteolysis. The 180-kD polypeptide (and any minor proteins) is not observed in similar protein samples prepared from a *spa2* mutant strain, *spa2-Δ1*, which is viable (see below). Thus, the *SPA2* gene encodes the 180-kD polypeptide.
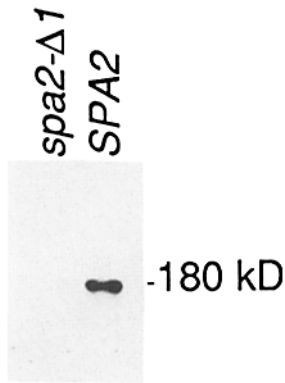
The SPA2 Gene Product Localizes to the Site of Bud Growth

Affinity-purified anti-SPA2 antibodies were next used as probes for indirect immunofluorescence using either a-cells, α-cells, or a/α-diploids. In budded cells of all three types,

Figure 4. Immunoblot of total yeast cellular proteins probed with affinity-purified anti–SPA2 antibodies. Total yeast cellular proteins were prepared from strain Y549 (wild-type) and Y550 (*spa2* mutant), and separated on a 5–16% gradient polyacrylamide gel containing SDS. Proteins were blotted to nitrocellulose and probed with affinity-purified anti–SPA2 antibodies. Comparable results were found using strains Y551 and Y548.

the SPA2 antigen is localized to a crescent at the tip of the bud, and in unbudded cells to a sharp crescent at one edge of the cell (Fig. 5, *A*, *C*, and *D*). No such staining is observed when either preimmune serum is used (not shown) or *spa2* mutant cells are used (Fig. 5 *F*).

Immunofluorescence experiments were also performed on cells whose growth was arrested with mating factors. a-Cells were treated with α-factor so that >95% of the cells arrested as unbudded cells; these cells were then probed with anti–SPA2 antibodies. The SPA2 antigen localized as a crescent at one apex of the cells as had been found for unbudded cells (Fig. 5 *E*). Moreover, many of the cells (40%) had acquired the pear-shaped cell morphology characteristic of "schmoos"; in these cells the SPA2 antigen localized to a crescent at the schmoo tip. The SPA2 reactivity was not seen in control experiments using isogenic a-*spa2* mutant cells treated with α-factor and was not present when preimmune serum was used (data not shown). A culture containing a-cells mixed with α-cells was also used for immunofluorescence with anti–SPA2 antibodies. Schmoos identified in this culture also stained the schmoo tip as before. In addition, budding zygotes showed staining at the tip of the newly formed bud. Thus, the SPA2 antigen localizes to a discrete site in growing and arrested cells and in all cell types.

Localization of the SPA2 Antigen in spa1 Mutant Cells

The *SPA1* gene of yeast was isolated with human anti–spindle pole autoantibodies and is involved in chromosome segregation and mitotic functions (Snyder and Davis, 1988). A large fraction of the population of *spa1* mutant cells (15–30%) contain more than one nucleus. When anti–SPA2 antibodies were used to probe *spa1* mutant cells, a staining pattern similar to that of wild-type cells was seen; in budded cells a crescent at the tip of the bud is observed, and in unbudded cells a crescent is found on one edge of the cell. However, ~10% of the cells that contain a single nucleus have more than one SPA2-localizing crescent (Fig. 5 *G*). In cells with multiple nuclei, >80% show aberrant SPA2 labeling; either a single enlarged crescent was seen or the numbers of crescents and nuclei were equal. For example, Fig. 5 *I* shows a cell with an apparently enlarged crescent, but careful inspection suggests that two crescents are present: one crescent is apparently half the size of a wild-type cell crescent, while the other is 1.5 times as large. Cells with multiple nuclei and SPA2 localization sites always have an equivalent number of spindle poles as determined using double immunofluores-

cence experiments with a human anti–microtubule antibody (Fig. 5 *K*; Snyder and Davis, 1988). Thus, *spa1* mutant cells exhibit alterations in the number and size of the SPA2-containing crescents, and in cells with multiple nuclei the number or size of the crescents correlates with the number of nuclei.

Disruption of the SPA2 Gene In Vivo

To investigate the function of the *SPA2* gene in vivo, disruption mutations were created by two different methods. Two mutant alleles, *spa2-7* and *spa2-8*, contain insertion mutations; these mutations were constructed in *E. coli* using mini-Tn10 transposable elements that contain the *URA3* gene (Snyder et al., 1986; Fig. 6). Subsequently, a large deletion allele, *spa2-Δ1*, was constructed by substituting a DNA fragment containing the *TRP1* gene for a 2.2-kb internal segment of *SPA2*. These alleles were transformed into diploid yeast cells.

When diploid strains heterozygous for *spa2-7*, *spa2-8*, or *spa2-Δ1* were sporulated, the internal marker (*URA3* or *TRP1*) segregated $2^+/2^-$ and haploid *spa2* mutant progeny were recovered at the same frequency as *SPA2* wild-type cells. *spa2* mutant colonies are equal in size to those of wild-type, and *spa2* cultures double in optical density at the same rate as wild-type cultures in rich media. Average cell division times are similar between *spa2* mutant and wild-type cells. Haploid *spa2* mutants mate well. Diploid *spa2/spa2* mutants complete meiosis successfully forming asci with four spores (see Discussion), and the spore viability is the same as for wild-type cells. Thus, *spa2* mutants appear similar in many respects to wild-type cells.

However, several phenotypes of *spa2* mutants can be observed; these phenotypes are similar, though not identical, for the *spa2-7*, *spa2-8*, and *spa2-Δ1* alleles. All of the *spa2* mutants have a higher proportion of budded cells than isogenic wild-type strains (88 vs. 74% for *spa2-7*; see below and Table III), and occasionally, cells with deformed buds are seen in growing cultures. *spa2* mutant cells often appear slightly smaller and rounder than isogenic wild-type cells. These phenotypes indicate that *SPA2* may play a role in the regulation of budding.

spa2 Mutants Have Slightly Altered Budding Patterns

spa2 mutants were next tested for defects in budding patterns. Individual cells were chosen from exponentially growing cultures by micromanipulation and the pattern of bud emergence in each growing cell was observed (see Materials and Methods). As described above, wild-type haploid cells exhibit an axial budding pattern; i.e., the new bud forms adjacent to the old bud site. This process is very accurate for mother cells; 124/124 cells underwent axial budding (Fig. 7; Table III). *spa2* mutant cells, however, occasionally deviate from this pattern; 3–15% of *spa2-7*, *spa2-8*, and *spa2-Δ1* haploid cells budded further than 90° from the old bud site. For daughter haploid cells similar results were observed; however, even in wild-type cells the accuracy of axial budding was reduced (see Materials and Methods).

For diploid cells the effect of the *spa2* mutation is much more pronounced, and the result varies slightly with the particular *spa2* allele. 78% of wild-type mother cells undergo an axial budding pattern. In contrast, diploid *spa2-7/spa2-7*
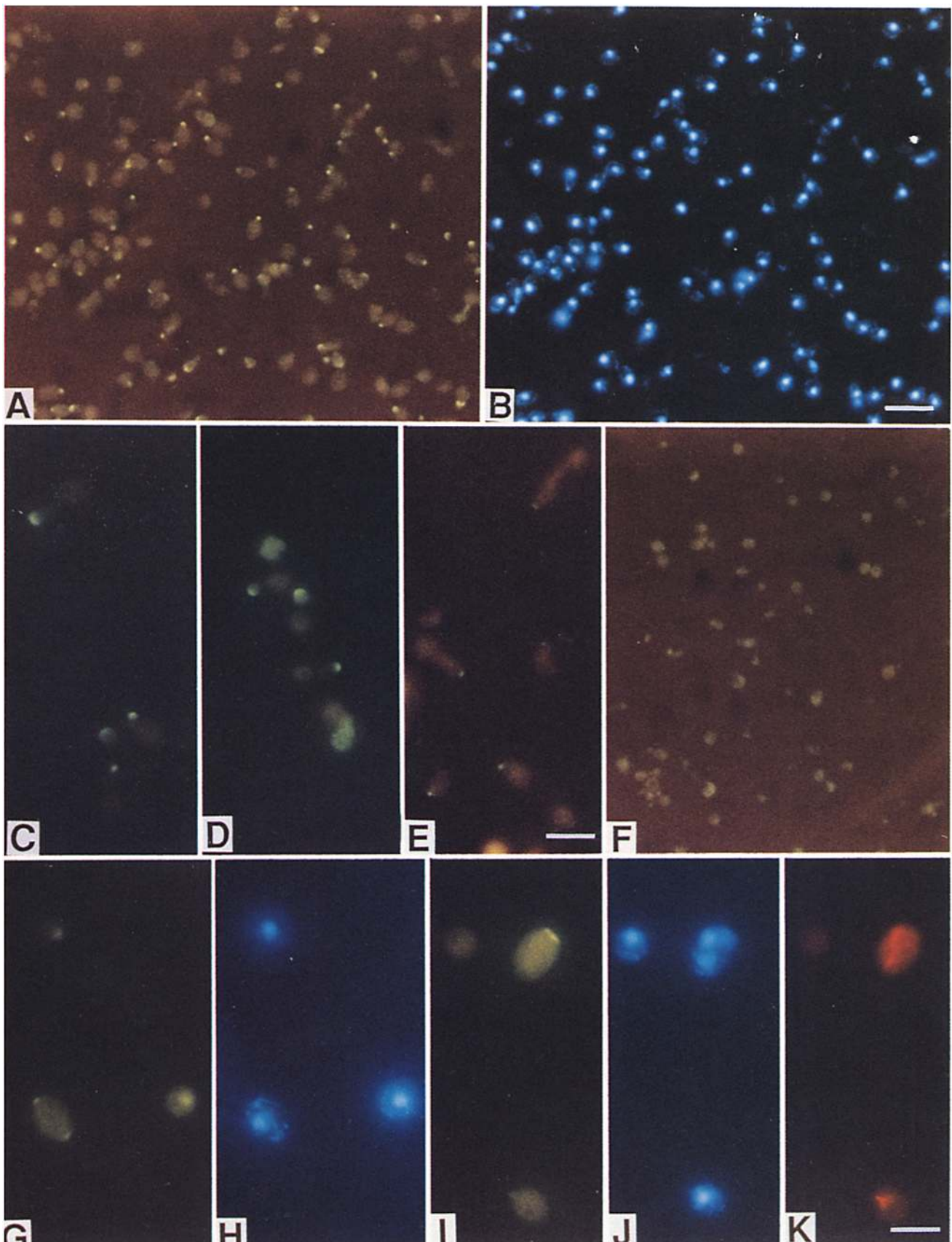
Figure 5. Immunofluorescence of yeast cells using anti–SPA2 affinity-purified antibodies. Indirect immunofluorescence was carried out as described in Materials and Methods; detection of bound antibodies was with fluorescein-conjugated second antibody probes. Cells were simultaneously stained with Hoechst 33258 to visualize the nucleus. (*A*) Diploid yeast cells (Y270) stained with anti–SPA2 antibodies. Greater than 80% of the unbudded cells show crescent labeling with these antibodies. (*B*) Hoechst stain of same sample. (*C*) Higher magnification of diploid cells stained with anti–SPA2 antibodies. (*D* and *E*) Haploid a-cells (Y133) treated with anti–SPA2 antibodies.
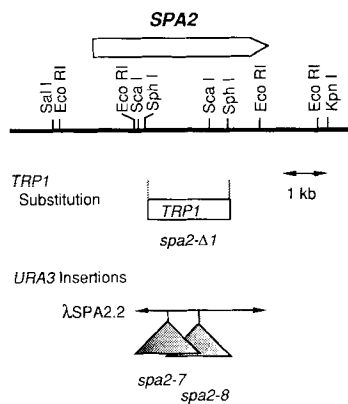
Figure 6. Location of the *spa2* insertion mutations and deletion mutation. Transplason insertion mutations containing the *URA3* gene in a mini-Tn10 transposon were generated in λ*SPA2.2* and substituted into the yeast genome to produce the indicated *spa2-7* and *spa2-8* alleles. The position of the insertions are indicated by the shaded triangles. The *spa2-Δ1* allele was constructed by substitution of a 1.4-kb *TRP1* DNA fragment for the internal 2.2-kb Sph I fragment of *SPA2*.

Table III. Effect of the spa2 Mutations on Budding Patterns

	<90°	>90°	R
	%	%	
Haploid Mothers			
wild-type	100	0	1.00
spa2-7	90	10	0.80
spa2-8	93	7	0.86
spa2-Δ1	97	3	0.94
Haploid Daughters			
wild-type	73	27	0.46
spa2-7	69	31	0.38
spa2-8	63	37	0.26
spa2-Δ1	63	37	0.26
Diploid Mothers			
wild-type	78	22	0.56
spa2-7	47	53	−0.06
spa2-Δ1	62	38	0.24
Diploid Daughters			
wild-type	20	80	−0.60
spa2-7	11	89	−0.78
spa2-Δ1	18	82	−0.64

Effect of the *spa2* mutations on budding patterns. The percentage of cells that budded <90° and >90° was determined as described in Fig. 7. As an additional means of analyzing these data, R values were calculated whereby $R = [(n \text{ of divisions} <90°) - (n \text{ of divisions} >90°)]/(\text{total } n \text{ of divisions})$. Thus 100% axial budding would yield $R = 1.0$, random budding would result in $R = 0.00$, and 100% polar budding would yield $R = -1.0$. This system of analysis is derived from that described for *Drosophila* olfaction assays (Rodrigues and Siddiqui, 1978).

mothers appear to bud randomly, so that only 46% bud <90° from the previous bud site and 54% bud >90° from the previous bud position. Diploid *spa2-Δ1/spa2-Δ1* mothers exhibit a reduced frequency of axial budding such that 62% bud <90° from the previous bud site. For diploid daughter cells, polar budding appears unaffected and perhaps is slightly increased by the presence of the *spa2* mutations (Fig. 7). Thus, *SPA2* is important for the direction of mother bud formation; haploid *spa2* mutants exhibit a minor defect in axial budding, while diploid mutants are more severely altered in this pattern.

spa2 Mutants Exhibit Defects in Cell Cycle Arrest Under Nutrient-limiting Conditions

Another phenotype of *spa2* mutants is an inability to arrest properly upon nutrient-limiting conditions. Isogenic *spa2-7/spa2-7* and wild-type diploid cultures were grown for 1, 2, or 3 d in rich medium, and the percentage of cells that contained buds was determined (Table IV). *spa2-7* and wild-type cell cultures were similar in both optical density and cell density at each time point. However, wild-type cells quickly stopped budding as the cultures became saturated, with only 27% of the cells containing buds after 27 h. In contrast, 60% of *spa2-7* cells remained budded. After 3 d, most *spa2* cells were unbudded, although the fraction containing buds (29%) was still higher than that of wild-type cells (17%). Interestingly, in cultures grown for either 1, 2, or 3 d, 36, 37, and 58%, respectively, of the budded *spa2-7* cells contained multiple buds, some possessing as many as six. Examples of cells with multiple buds are shown in Fig. 8. Under these conditions <10% of budded wild-type cells contained more than one bud.

As an alternative assay for entry into stationary phase, the resistance of *spa2* mutants to heat shock was tested (see Whiteway and Szostak, 1985). Logarithmically growing yeast cells die when suddenly exposed to high temperatures, but cells in stationary phase are resistant (Table IV). Exponentially growing cultures of *spa2-7*, *spa2-Δ1*, and wild-type diploid cells were incubated for 0, 1, 2, or 3 d as described above and briefly shifted to 54.5°C. The frequency of viable cells was then determined relative to that of cells that did not receive a heat shock. For each time point, the percentage of *spa2* mutant cells that survived the heat shock was less than that of wild-type cells (Table IV). For example, in wild-type cultures after 3 d of growth, 70% of the cells were resistant to heat shock; however, in *spa2-7* mutant strains only 39% were resistant. Thus, *spa2* mutants often have problems entering stationary phase under nutrient-limiting conditions, and many *spa2-7* cells accumulate more than one bud under these conditions.

Discussion

A gene was isolated from *S. cerevisiae* using human anti-spindle pole antibodies and named *SPA2*. *SPA2* may play an important role in bud formation and cell growth. Consistent with this suggestion, the SPA2 protein localizes to the site of

In *E*, the a-cells had been arrested with α-factor. (*F*) *spa2-7* homozygous diploids stained with anti–SPA2 antibodies. *spa2* mutant cells are typically slightly smaller than that of wild-type cells; this experiment shows an extreme example. (*G* and *I*) *spa1-1* homozygous diploid cells (Y376) stained with anti–SPA2 antibodies. Note the double crescent in *G* and enlarged crescent in *I*, respectively. (*H* and *J*) Hoechst stains of the same samples. For the cell shown in *G*, the mitochondria are near the crescents. (*K*) Anti-microtubule stain of the sample in *I* and *J* detected with rhodamine probes. The two arrays of microtubules were not in the same plane of focus, and a best-attempt photograph is presented. Bars: (*A, B*, and *F*) ∼15 μm; (*C-E* and *G-K*) ∼6 μm.

Figure 7. Direction of budding of *spa2* mutant and wild-type cells. The budding pattern of new mother cells and daughter cells was determined by observation of individual cell growth on plates using a dissection microscope (see Materials and Methods). The direction of the new bud was determined relative to the old bud site for each cell. The ordinate refers to the percentage of yeast cells that exhibit the pattern indicated on the axis. For simplicity, the results are presented as <90° or >90°; subdivision of the budding patterns into 45° or 60° intervals yields similar conclusions. The number of cell divisions observed was 118–184 (mean 137). See also Table III.

Table IV. Tests for Entry into Stationary Phase

	Budded cells		Survival after heat shock				
			Experiment 1		Experiment 2		
Hours	spa2-7	Wild-type	spa2-7	Wild-type	spa2-Δ1	Wild-type	Days
	%	%	%	%	%	%	
0	88	74	0.01	0.01	0.01	0.02	0
27.5	60	27	9.0	18	7.7	13.5	1
47	34	27	34	55	22	42	2
71	29	17	39	69	35	84	3
	nt	nt	nt	nt	42	92	4

Tests for entry of *spa2* cells into stationary phase. *spa2-7* (Y457) and wild-type (Y270) diploid cells were grown logarithmically in YPD diluted to OD (600) = 0.025 and incubated for 0, 27.5, 47, or 71 h without dilution (*Budded cells*). At each time point the OD (600) was slightly higher (8–20%) for the *spa2* mutant cultures relative to wild-type cultures. The percentage of *spa2-7* and wild-type cells that contained buds was scored by light microscopy (190–400 cells were scored at each interval). In similar experiments with *spa2-Δ1* cells, the percentage of budded cells resembles that of wild-type cells. Aliquots of cells were diluted to 0.5×10^6 cells/ml and subjected to a 5-min heat shock at 54.5°C. Aliquots were plated in duplicate on YPD plates and the number of viable cells determined relative to an untreated sample. For *Experiment 1*, the time points were as described above. *nt*, not tested. For *Experiment 2*, the time points were 0, 26, 50, 74, and 103 h (for each sample 211–1,166 viable colonies were scored. Mean, 435).

bud growth in budding cells, and to a discrete crescent on the edge of unbudded cells. In unbudded cells SPA2 may mark the site where bud formation will occur; the SPA2 protein resides at one end of the cell, and in a-cells arrested with α-factor the SPA2 crescent is found at the schmoo tip. The schmoo tip has been reported as the site of bud formation upon hormone removal (for example, see Holm et al., 1985). Actin is also in these regions in budded and unbudded cells, but with a pattern very different from SPA2 (Adams and Pringle, 1984; Kilmartin and Adams, 1984).

Mutations were constructed in the *SPA2* gene using transplason insertions (Snyder et al., 1986) and standard deletion–substitution methods. These mutations are still capable of making truncated *spa2* polypeptides and are not necessarily null mutations. Assuming 180 kD is a reasonable size estimate of the primary SPA2 translation product, then the maximum amount of functional *SPA2* coding sequence 5' to the disruption is ~1.5, 1.9, and 3.3 kb for the *spa2-Δ1*, *spa2-7*, *spa2-8* alleles, respectively. Thus, for *spa2-Δ1* the maximum size of any truncated polypeptide is expected to be less than one third the length of the wild-type gene product.

spa2 mutants are viable but exhibit defects in budding and in the control of cell growth. Under nutrient-limiting conditions, *spa2* cells have difficulty entering into stationary phase, and *spa2-7* cells synthesize multiple buds. In exponentially growing cultures occasional cells are observed that have deformed buds. *spa2* mutants are typically slightly smaller and rounder than their wild-type counterparts, and a higher fraction of *spa2* mutants cells are budded. Phenotypes involving budding and growth control are not unexpected from mutagenesis of a single gene, because bud formation is linked with initiation of a new cell cycle, and these events are presumably coordinately controlled. Therefore, defects in either pathway, budding or cell cycle control, may directly or indirectly perturb the other pathway.

Impaired entry into stationary phase is a phenotype *spa2*

mutants share with *ard1* and *bcy1* mutants, although the defect appears to be a more severe for *ard1* and *bcy1* cells than for *spa2* mutants. The *BCY1* gene encodes the regulatory subunit of cAMP-dependent protein kinase, and the *ARD1* gene encodes a potential DNA-binding protein with some sequence similarity to the homeobox (Toda et al., 1985; Whiteway and Szostak, 1985). At present, the gene products acted upon by the cAMP-dependent protein kinase and ARD1 protein are unknown. It will be interesting to determine whether the SPA2, ARD1, and BCY1 proteins all operate in the same pathway. Like *ard1* and *bcy1* mutants, *spa2-Δ1* mutants typically form fewer four-spored tetrads than wild-type cells (data not shown). Interestingly, *spa2* tetrads that have formed frequently contain a bud adjacent to the ascus suggesting that they have undergone meiosis before the proper arrest of mitotic cell growth.

In addition to a role in cell cycle control, *SPA2* affects the budding pattern of yeast cells. *spa2* mutants sometimes deviate from the expected axial budding pattern in haploids. In diploids, *spa2* mother cells exhibit a reduced fidelity of axial budding; in fact, *spa2-7* mutants bud randomly. Thus, a SPA2-dependent mechanism must affect the fidelity of axial budding of diploid mother cells. In *spa2* diploids, the polar budding pattern of daughter cells is not disturbed. The effect of the *spa2* mutation may be to impair the overall fidelity of axial budding. Because the efficiency of axial budding in mothers is poor in diploid cells relative to haploid cells (78 vs. 100%, respectively), the defect may therefore appear more pronounced in diploids.

In general, the budding defects of *spa2-7* mutants appear stronger than those of *spa2-Δ1* cells. It is therefore possible that a residual *spa2-7* gene product may interfere with normal budding functions.

The protein encoded by *SPA2* is antigenically related to the mammalian spindle pole; the significance of this observation is unclear. The SPA2 protein may fortuitously contain an epitope cross-reactive with the mammalian spindle pole. This epitope is probably not frequently recognized by anti–spindle pole autoantibodies because only one of four sera tested reacted with *SPA2* λgt11 clones (Snyder and Davis, 1988). An alternative, but potentially more interesting, possibility is that SPA2 may be involved in microtubule capture. In yeast cells, double immunofluorescence experiments with anti-microtubule and anti–SPA2 antibodies indicate that the SPA2 crescent usually resides on the same side of the nucleus as the spindle pole; this configuration would be expected if the SPA2 protein were at one end of the cytoplasmic microtubule bundle (Byers, 1981). In cells that do contain long extranuclear microtubule bundles, the distal end of the bundle (the presumed plus end) is always observed to intersect the SPA2 crescent (Page, B., and M. Snyder, unpublished observations). That SPA2-related polypeptides interact either directly or indirectly with microtubules in other eukaryotes is suggested by the fact that, in frog neurons, anti–SPA2 antibodies react well with a protein in neurites (Snyder, M., unpublished observations); neurites contain copious amounts of microtubules.

In *spa1* mutant cells with multiple nuclei, the number of SPA2 crescents correlates with the number of nuclei present. It is possible that the number of nuclei (and perhaps spindle poles) directly or indirectly determines the number of SPA2 crescents. The SPA2 patches could in turn affect the number
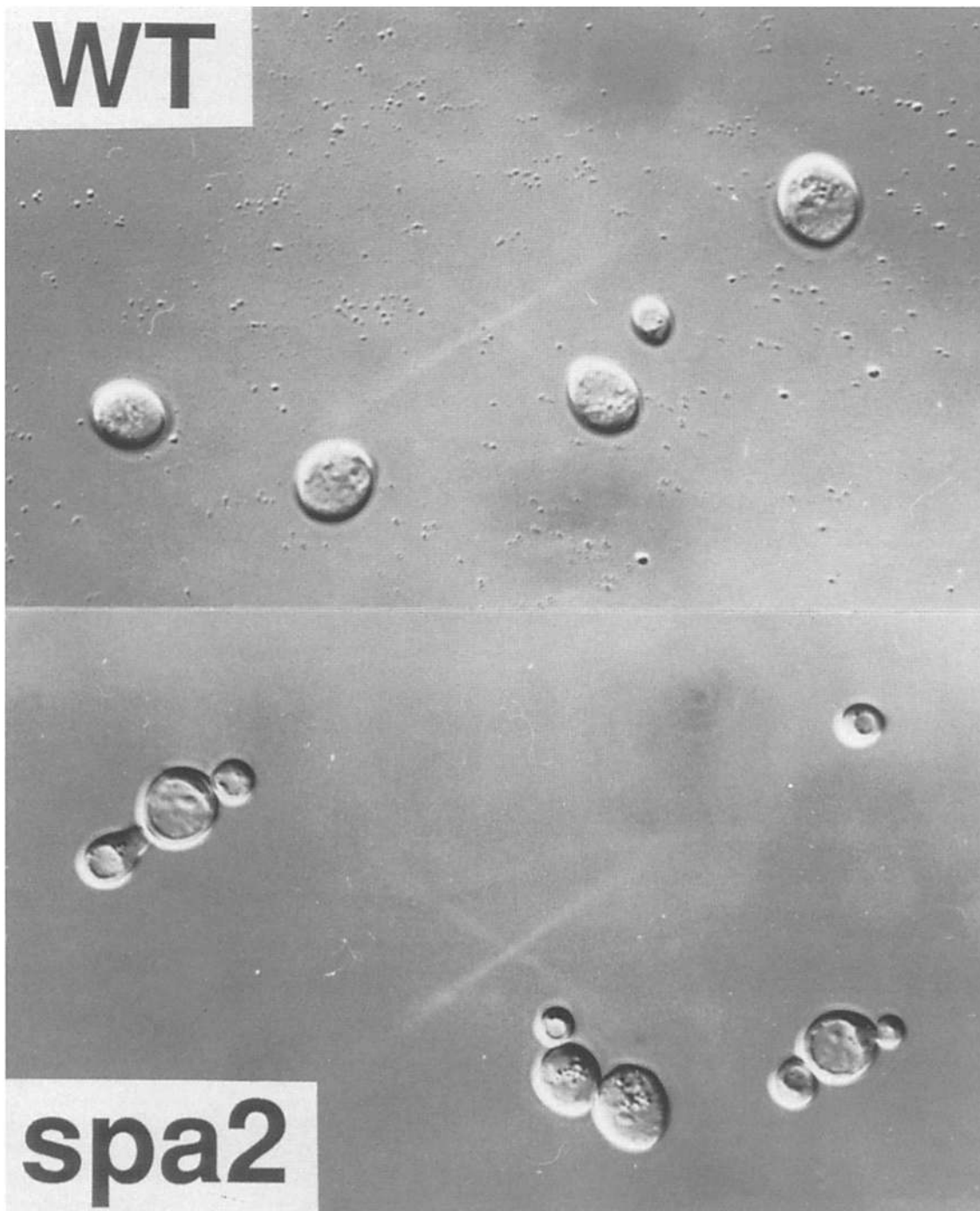
Figure 8. spa2-7 mutant cells often contain multiple buds under nutrient-limiting conditions. spa2-7/spa2-7 (Y457) and wild-type (Y270) diploid cells were grown 27.5 h in YPD media and viewed using Nomarski interference microscopy.

of buds formed since spa1 mutant cells that contain multiple nuclei often contain multiple buds (Snyder and Davis, 1988).

Attempts to make spa1/spa2 double mutants through simple genetic crosses have been unsuccessful. Diploid cells heterozygous or homozygous for the spa1 mutation sporulate well, as do spa2 diploids. However, spa1/spa2 double heterozygotes rarely form four-spored tetrads. The sporulation defect of spa1/spa2 double heterozygotes suggests that both genes may be involved in similar pathways or similar functions.

The SPA2 protein localizes to sites of yeast cell growth and plays a role in determining the direction of cell division. The CDC24 gene product of yeast is also involved in bud formation and in establishing the direction of cell growth (Sloat et al., 1981). J. Chant and I. Herskowitz (personal communication) have identified five additional genes important for directing axial budding in haploid yeast cells. Further analysis of yeast genes involved in polarized growth and division may allow an understanding of the molecular mechanisms by which eukaryotes carry out these fundamental processes.

1428

References

Adams, A. E. M., and J. R. Pringle. 1984. Relationship of actin and tubulin distribution to bud growth in wild-type and morphogenetic-mutant *Saccharomyces cerevisiae. J. Cell Biol.* 98:934-945.

Baker, T. A., A. D. Grossman, and C. A. Gross. 1984. A gene regulating the heat shock response in Escherichia coli also affects proteolysis. *Proc. Natl. Acad. Sci. USA.* 81:6779-6783.

Bond, J. F., J. L. Fridovich-Keil, L. Pillus, R. C. Mulligan, and F. Solomon. 1986. A chicken-yeast chimeric b-tubulin protein is incorporated into mouse microtubules in vivo. *Cell.* 44:461-468.

Burnette, W. N. 1981. "Western blotting": electrophoretic transfer of proteins from sodium dodecyl sulfate-polyacrylamide gels to unmodified nitrocellulose and radiographic detection with antibody and radioiodinated protein A. *Anal. Biochem.* 112:195-203.

Byers, B. 1981. Cytology of the yeast life cycle. *In* The Molecular Biology of the Yeast Saccharomyces: Life Cycle and Inheritance. J. N. Strathern, E. W. Jones, and J. R. Broach, editors. Cold Spring Harbor Laboratory, Cold Spring Harbor, New York. 59-96.

Byers, B., and L. Goetsch. 1975. Behavior of spindles and spindle plaques in the cell cycle and conjugation of Saccharomyces cerevisiae. *J. Bacteriol.* 124:511-523.

Davis, R. W., D. Botstein, and J. R. Roth. 1980. Advanced Bacterial Genetics. Cold Spring Harbor Laboratory, Cold Spring Harbor, NY. 254 pp.

Freifelder, D. 1960. Bud position in *Saccharomyces cerevisiae. J. Bacteriol.* 80:567-568.

Hartwell, L. H. 1974. *Saccharomyces cerevisiae* cell cycle. *Bacteriol. Rev.* 38:164-198.

Holm, C., T. Goto, J. C. Wang, and D. Botstein. 1985. DNA topoisomerase II is required at the time of mitosis in yeast. *Cell.* 41:553-563.

Huffaker, T. C., J. H. Thomas, and D. Botstein. 1988. Diverse effects of β-tubulin mutations on microtubule formation and function. *J. Cell Biol.* 106: 1997-2010.

Ito, H., Y. Fukuda, K. Murata, and A. Kimura. 1983. Transformation of intact yeast cells treated with alkali cations. *J. Bacteriol.* 153:163-168.

Jacobs, C. W., A. E. M. Adams, P. J. Szaniszlo, and J. R. Pringle. 1988. Functions of microtubules in the *Saccharomyces cerevisiae* cell cycle. *J. Cell Biol.* 107:1409-1426.

Kilmartin, J. V., and A. E. M. Adams. 1984. Structural rearrangements of tubulin and actin during the cell cycle of the yeast *Saccharomyces. J. Cell Biol.* 98:922-933.

Laemmli, U. K. 1970. Cleavage of structural proteins during the assembly of the head of bacteriophage T4. *Nature (Lond.).* 227:680-685.

Maniatis, T., E. F. Fritsch, and J. Sambrook. 1982. Molecular Cloning: A Laboratory Manual. Cold Spring Harbor Laboratory, Cold Spring Harbor, NY. 545 pp.

Mortimer, R. K., and D. Schild. 1980. Genetic map of *Saccharomyces cerevisiae. Microbiol. Rev.* 44:519-571.

Pringle, J. R., and L. H. Hartwell. 1981. The *Saccharomyces cerevisiae* cell cycle. *In* The Molecular Biology of the Yeast *Saccharomyces*: Life Cycle and Inheritance. J. N. Strathern, E. W. Jones, and J. R. Broach, editors. Cold Spring Harbor Laboratory, Cold Spring Harbor, NY. 97-142.

Rothstein, R. J. 1983. One-step gene disruption in yeast. *Methods Enzymol.* 101:202-211.

Rodrigues, V., and O. Siddiqi. 1978. Genetic analysis of chemosensory pathway. *Proc. Indian Acad. Sci. Sect. B.* 87:147-160.

Sherman, F., G. Fink, and J. Hicks. 1986. Methods in Yeast Genetics. Cold Spring Harbor Laboratory, Cold Spring Harbor, NY. 186 pp.

Sloat, B. F., A. Adams, and J. F. Pringle. 1981. Roles of the *CDC24* gene product in cellular morphogenesis during the *Saccharomyces cerevisiae* cell cycle. *J. Cell Biol.* 89:395-405.

Snyder, M., and R. W. Davis. 1988. SPA1: a gene important for chromosome segregation and other mitotic functions in *Saccharomyces cerevisiae. Cell.* 54:743-754.

Snyder, M., S. Elledge, and R. W. Davis. 1986. Rapid mapping of antigenic coding regions and constructing insertion mutations in yeast genes by mini-Tn10 mutagenesis. *Proc. Natl. Acad. Sci. USA.* 83:730-734.

Snyder, M., S. Elledge, D. Sweetser, R. Young, and R. W. Davis. 1987. λgt11: gene isolation with antibody probes and other applications. *Methods Enzymol.* 154:107-128.

Toda, T., I. Uno, T. Ishikawa, S. Powers, T. Kataoka, D. Broek, S. Cameron, J. Broach, K. Matsumoto, and M. Wigler. 1985. In yeast, RAS proteins are controlling elements of adenylate cyclase. *Cell.* 40:27-36.

Tuffanelli, D. L., F. McKeon, D. M. Kleinsmith, T. K. Burnham, and M. Kirschner. 1983. Anticentromere and anticentriole antibodies in the scleroderma spectrum. *Arch. Dermatol.* 119:560-566.

Whiteway, M., and J. W. Szostak. 1985. The *ARD1* gene of yeast functions in the switch between the mitotic cell cycle and alternate developmental pathways. *Cell.* 43:483-492.